Design of high-sensitivity metal-coated LPFG sensor based on material dispersion*

SHI Yan-jun(石彦军) **and GU Zheng-tian**(顾铮天)**

Laboratory of Photoelectric Functional Films, University of Shanghai for Science and Technology, Shanghai 200093, China

(Received 22 March 2012)

A high-sensitivity metal-coated long-period fiber grating (LPFG) sensor based on material dispersion is designed. Based on the coupled mode theory, the influence of the material dispersion on the dual-peak characteristics of the metal-coated LPFG is studied. After considering the material dispersion, the jumping region of the dual-resonant-wavelength shifts toward the thinner film thickness, and the sensitivity of the dual-peak metal-coated LPFG sensor to liquid refractive index (RI) can be obtained to supply accurate parameter combinations. Experimentally, two kinds of silver-coated LPFGs with different film thicknesses and grating periods are fabricated to monitor the salt solution, and the sensitivities of these two sensors are compared. The experimental results are consistent with the theoretical analyses.

Document code: A **Article ID:** 1673-1905(2012)04-0269-4

DOI 10.1007/s11801-012-2001-7

The long-period fiber grating (LPFG) has a wide range of applications in optical communications and sensing systems, such as band rejection filters[1] and liquid level measurements[2]. In recent years, the sensor based on the LPFG coated with the noble metal nano-layers, such as gold and silver, has rapidly emerged as an excellent refractive index (RI) sensor for chemical and biological sensing[3,4]. These LPFG sensors have considerable advantages, including the extraordinary optical properties (e.g., absorbance) of gold colloidal nano-particles[5] and an enhancement of chemical sensitivity[6-8]. Huai Wei et al[9] investigated the influence of metal layer on the transmission spectrum of metal-coated LPFG based on vector analysis, and found that the experimental results agree well with the theoretical analyses. Mitsuhiro Iga et al[10] reported the effect of gold film thickness on the sensitivity of gold-coated optical fiber sensor. The sensitivity can be optimized by controlling the thickness of gold film. Furthermore, in Refs.[9,10], the experimental transmission spectra accord with the theoretical analyses, but there exists deviation in the resonant wavelength, which is probably due to the model error and the approximation. In our opinion, the influence of the material dispersion is also an important factor.

In addition, Tang et al[11] presented an RI LPFG sensor coated with Au film for label-free detection of bio-molecular, and pointed out that the sensitivity of the sensors is low, which can be enhanced by the optimization of some key parameters. A. Iadicicco et al[12] reported an LPFG coated with nano-scale gold, and discovered that the LPFG sensor can exhibit a shielding effect for the specific surrounding RI (SRI) ranging from 1.32 to 1.40, which indicated that this sensor is insensitive to the SRI. The sensitivity of the coated LPFG sensor is closely related to the film thickness and grating parameters, so the influence of the material dispersion can not be neglected in the design of high-sensitivity metal-coated LPFG sensor.

In this paper, the influence of the material dispersion on the resonant characteristics of the metal-coated LPFG is analyzed based on the coupled mode theory. Before and after considering the material dispersion, the jumping region of the resonant wavelength to the metal film thickness is investigated. Then the sensitivity for SRI is discussed based on material dispersion. In the experiment, two silver-coated LPFG sensors with different film thicknesses and grating periods are prepared, and their responses to the salt solution are observed. The experimental results indicate that it is necessary to consider the influence of material dispersion in the

* This work has been supported by the National Natural Science Foundation of China (No.60777035), the Scientific Research Key Project Fund (No. 208040), the Innovation Program of Shanghai Municipal Education Commission (No.11ZZ131), and the Shanghai Leading Academic Discipline Project (No.S30502).

** E-mail: zhengtiangu@163.com

optimization design of high-sensitivity metal-coated LPFG sensor.

Fig.1 shows the structural diagram of the metal-coated LPFG with four layers. The metal material is silver. The refractive indices of fiber core, cladding, silver film and surrounding medium are n_1, n_2, n_3, n_4, respectively. a_1, a_2 and a_3 represent the radii of fiber core, cladding and silver film, respectively. n_1, n_2 and n_3 are 1.4682, 1.4628 and 0.469+9.32i at the wavelength of 1550 nm, respectively. a_1 and a_2 are 4.15 μm and 62.5 μm. The thickness of silver film h_3 is 50 nm. The length of the grating is 1 cm. The grating period is Λ. The modulation is σ with the amplitude of 10^{-4}.

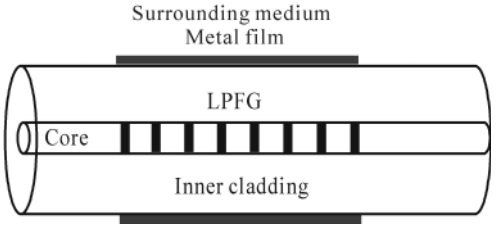

Fig.1 Schematic diagram of the metal-coated LPFG with four layers

The dual resonant wavelengths can be determined by[13]:

$$n_{\text{eff,co}}(\lambda) - n^{\nu}_{\text{eff,cl}}(\lambda) = \frac{\lambda}{\Lambda}, \quad \nu = 1,2,3,\cdots , \tag{1}$$

where $n_{\text{eff,co}}(\lambda)$ and $n^{\nu}_{\text{eff,cl}}(\lambda)$ are the effective refractive indices of the core fundamental mode and the ν th cladding mode, respectively. λ is the resonant wavelength corresponding to the ν th cladding mode.

Due to the single mode fiber uses conventional GeO_2-doped SiO_2 as core and pure SiO_2 as cladding, the refractive index of the core is 0.0050−0.0055, which is higher than that of the cladding[14]. When the wavelength changes from 0.2 μm to 4.0 μm, the approximate calculation of the refractive index of the cladding is expressed as[15]:

$$n_2^2 - 1 = \frac{0.6961663\lambda^2}{\lambda^2 - (0.068403)^2} + \frac{0.4079426\lambda^2}{\lambda^2 - (0.1162414)^2} + \frac{0.8974794\lambda^2}{\lambda^2 - (9.89616)^2} . \tag{2}$$

The refractive index of fiber core increases by σ after UV irradiation, and the approximate calculation of the refractive index of core is expressed as:

$$n_1 = n_2 + 0.0052 + \sigma . \tag{3}$$

According to the discrete data[16], the approximate calculation equations of the refractive index and extinction coefficient of silver are derived through least squares fitting method, respectively:

$$n_3(\lambda) = -1.6578 \times 10^{11} \cdot \lambda^2 + 9.430 \times 10^5 \cdot \lambda - 0.57721 , \tag{4}$$

$$\kappa_3(\lambda) = 2.9670 \times 10^{11} \cdot \lambda^2 - 3.0830 \times 10^{11} \cdot \lambda + 7.2079 . \tag{5}$$

In Fig.2, it is evident that the dual resonance peaks shift in opposite directions with the increase of SRI, no matter the material dispersion is considered or not. Without regarding the material dispersion, the interval of dual resonance peaks changes from 460 nm to 510 nm with the increase of SRI from 1.33 to 1.36. The change of the dual resonance peak interval is 50 nm. While considering the material dispersion, under the same variation of the SRI, the change of the dual resonance peak interval is 43 nm. Therefore, the material dispersion has relatively obvious influence on the transmission characteristics of metal-coated LPFG.

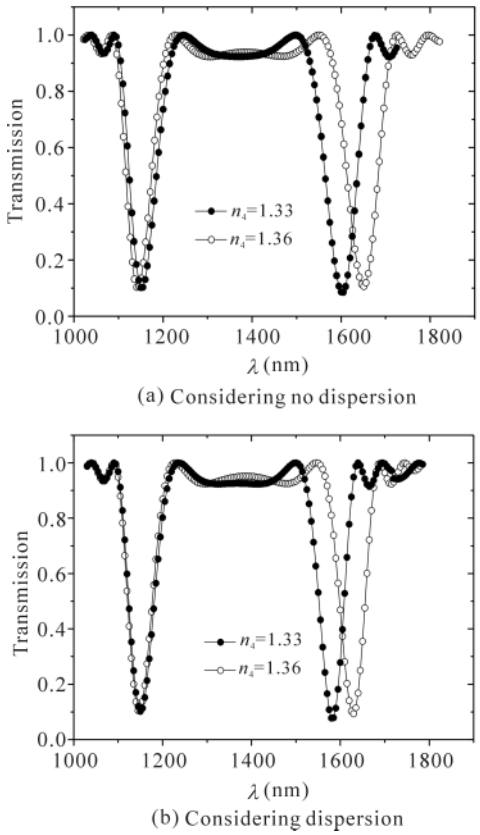

Fig.2 Transmission spectra of the $EH_{1,10}$ cladding mode under different SRI values

Ref.[17] pointed out there is a jumping region of the resonant wavelength to the thin film thickness, in which the resonant wavelength disappears and there is abnormal phenomenon in the transmission spectrum. Fig.3 shows the transmission spectrum of the $EH_{1,10}$ cladding mode before and after considering the material dispersion when the grating period is 177 μm and the metal film thickness is 101 nm. The transmission spectrum becomes abnormal while considering the material dispersion.

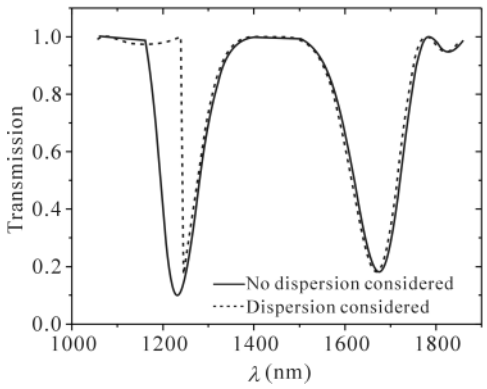

Fig.3 Transmission spectra of the $EH_{1,10}$ cladding mode around the jumping region

Fig.4 shows the dependence of the dual resonant wavelength on the metal film thickness before and after considering the material dispersion. It contains two distinct jumping regions. Without regarding the material dispersion, there exists a jumping region with the silver film thickness of 105 nm–167 nm. While considering material dispersion, the jumping region is broadened and located in the range of 97 nm–166 nm. Therefore the material dispersion should be taken into consideration to avoid the dual resonant wavelengths located in the jumping region.

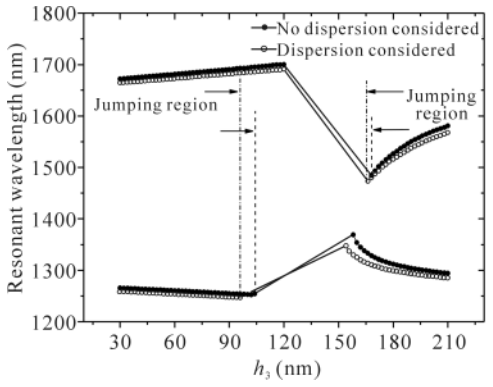

Fig.4 Relation between resonant wavelength and silver film thickness

The sensitivity S_n of the dual-peak metal-coated LPFG sensor is expressed by the variation of the dual resonance peak interval $\Delta\lambda$ with the SRI of n_4.

Fig.5 shows the dependence of the $S_{n|\max}$ on the metal film thickness and liquid RI when grating parameters are fixed, where $S_{n|\max}$ represents the maximum of S_n in the common observed wavelength range of 1000−1700 nm. It can be seen from Fig.5 that the sensitivity changes greatly while considering material dispersion. In addition, the $S_{n|\max}$ of blank space is zero, which indicates there is no dual resonance peak for the given combinations of n_4 and h_3, so the blank spaces should be avoided. For the specific liquid RI, the high sensitivity can be obtained by adjusting the film thickness controlled by coating technology.

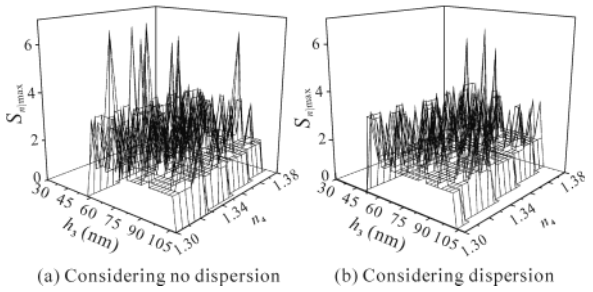

Fig.5 Dependence of $S_{n|\max}$ on h_3 and n_4

From Fig.6, it indicates explicitly that there is a great difference in the $S_{n|\max}$ for the same parameter combination of h_3 and Λ before and after considering the material dispersion. Without regarding the material dispersion, the $S_{n|\max}$ is 6.6 when Λ is 178.6 μm and h_3 is 60 nm. While considering the material dispersion, the $S_{n|\max}$ is only 1.36 under the same parameters.

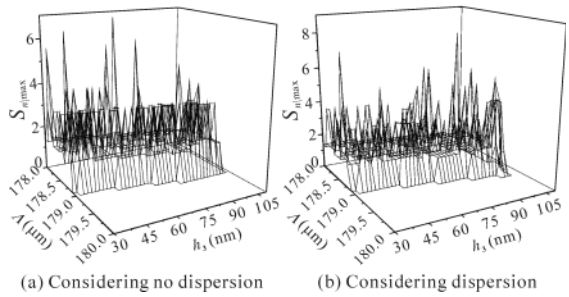

Fig.6 Dependence of $S_{n|\max}$ on h_3 and Λ

In order to verify that it is necessary to consider the material dispersion in the optimization design of high sensitivity metal-coated LPFG sensor, we prepared two silver-coated LPFGs with different grating periods and silver film thicknesses. The fiber used in the experiment is Corning SMF-28 which was hydrogen loaded for one month in 150 atm of hydrogen with high purity to enhance its photosensitivity. The grating period is determined by the step length of the precise moving platform controlled by a computer. Silver films were deposited on LPFG by adopting DC sputtering. The first LPFG (L1) is with the silver thickness of 40.9 nm and the grating period of 178.5 μm. The second one (L2) is with the silver thickness of 103 nm and the grating period of 179 μm.

For liquid sensing, the salt solutions with concentration of 1%−25% were prepared. The refractive indices were measured with a WAY-IS Abbe refractometer. The LPFG was illuminated by a broadband stable light source (OS310062), and the transmission spectra were captured on an optical spec-

trum analyzer (AQ6370). The positions of the dual resonance peaks were observed under different concentrations of salt solution.

To compare the responses of L1 and L2 to the salt solution, the interval changes of the dual resonance peaks of L1 and L2 under different concentrations of the salt solution are listed in Tab.1. As the salt solution concentration increases from 1% to 25%, the dual resonance peaks are far away from each other. For the L1, the left resonant wavelength λ_1 shifts by about 6.2 nm towards the shorter wavelength, and the right resonant wavelength λ_2 shifts by about 10.6 nm towards the longer wavelength. The interval change $\Delta\lambda$ of dual resonance peaks is 16.8 nm. For the L2, the left resonant wavelength λ'_1 shifts by 18.6 nm towards the shorter wavelength, and the right resonant wavelength λ'_2 shifts by about 29.8 nm towards the longer wavelength. The interval change $\Delta\lambda'$ of dual resonant peaks is 48.4 nm, which is almost three times of that of L1. It implies that the sensitivity to liquid RI of L2 is higher than that of L1.

Tab.1 Interval changes of dual peaks of L1 and L2 under different concentrations of salt solution

Concentration (%)	Refractive index n	L1		Interval change $\Delta\lambda$ (nm)	L2		Interval change $\Delta\lambda'$(nm)
		λ_1 (nm)	λ_2(nm)		λ'_1(nm)	λ'_2(nm)	
1	1.3352	1321.8	1668.6		1356.8	1660.2	
5	1.3424	1321.0	1670.0	2.2	1353.0	1670.2	13.8
10	1.3510	1320.4	1672.2	2.8	1349.4	1676.8	10.2
15	1.3609	1319.8	1673.2	1.6	1345.8	1681.2	8.0
20	1.3708	1317.8	1676.6	5.4	1342.0	1685.2	7.8
25	1.3792	1315.6	1679.2	4.8	1338.2	1690.0	8.6

Theoretically, for the metal-coated LPFG sensor with the fixed grating parameters and metal film thickness, it has different sensitivities for different liquid RI values from 1.3 to 1.4, as is described in Fig.5. From Fig.6, we can see that without regarding the material dispersion, the $S_{n|\max}$ of L1 is 2.98, the $S_{n|\max}$ of L2 is 2.84, and they are almost equal to each other. While considering the material dispersion, the $S_{n|\max}$ of L2 (4.93) is about three times of the $S_{n|\max}$ (1.36) of L1, which results in the larger interval change of dual resonance peaks of L2. Therefore, the theoretical analyses on the sensitivity while considering the material dispersion are in accordance with the experimental results.

In summary, the design of high-sensitivity dual-peak metal-coated LPFG sensor based on material dispersion consideration is presented. Influenced by the material dispersion, the jumping region of the dual resonant wavelengths to metal film thickness is broadened and shifts towards the thinner silver film thickness. The optimal parameters with considering material dispersion can be easily obtained by analyzing the relationship among the sensitivity, the metal film thickness and the grating parameters. The liquid-sensing experimental results accord with the theoretical analyses based on material dispersion consideration. So it is necessary to consider the material dispersion in the design of high-sensitivity metal-coated LPFG sensor.

References

[1] Xiaoqin Li, Yong Zhu, Hao Mei, Chao Wang and Wei Wei, Journal of Optoelectronics • Laser **22**, 980 (2011). (in Chinese)

[2] Jinting Zhao, Zhengrong Tong, Xiufeng Yang, Hui Yu and Bin Yao, Journal of Optoelectronics • Laser **21**, 1777 (2010). (in Chinese)

[3] Rajneesh K. Verma and Banshi D. Gupta, J. Opt. Soc. Am. A **27**, 846 (2010).

[4] Yu-Chun Lu, Wei-Ping Huang and Shui-Sheng Jian, Journal of Lightwave Technology **27**, 4804 (2009).

[5] Jaw-Luen Tang and Jien-Neng Wang, Sensors **8**, 171 (2008).

[6] Yanina Y. Shevchenko and Jacques Albert, Optics Letters **32**, 211 (2007).

[7] Kuei-Chu Hsu, Nan-Kuang Chen, Cheng-Ling Lee, Yu-Syun Chih, Pei-Jhuang, Yinchieh Lai and Chinlon Lin, Journal of Lightwave Technology **28**, 1057 (2010).

[8] Tobias Schuster, Reinhold Herschel, Niels Neumann and Christian G. Schaffer, Journal of Lightwave Technology **30**, 1003 (2012).

[9] Huai Wei, Zhi Tong, Muguang Wang and Shuisheng Jian, Acta Optic Sinica **23**, 931 (2003). (in Chinese)

[10] Mitsuhiro Iga, Atsushi Seki and Kazuhiro Watanabe, Sensors and Actuators B **106**, 363 (2005).

[11] Jaw-Luen Tang, Shu-Fang Cheng, Wei-Ting Hsu, Tsung-Yu Chiang and Lai-Kwan Chau, Sensors and Actuators B **119**, 105 (2006).

[12] A. Iadicicco, S. Campopiano, D. Paladino, A. Cutolo, A. Cusano and W. Bock, Sensors and Microsystems: AISEM 2009 Proceedings, 133 (2009).

[13] Turan Erdogan, J. Opt. Soc. Am. A **14**, 1760 (1997).

[14] Li Min, Liao Yanbiao and Shi Chunzheng, Acta Photonica Sinica **29**, 171(2000). (in Chinese)

[15] Yuquan Li and Min Cui, Optical Waveguide Theory and Technology, 1st ed, Beijing: Posts & Telecommunications Press, 157 (2002). (in Chinese)

[16] Edward D. Palik, Handbook of Optical Constants of Solids, 1st ed, New York: Academic Press, 350 (1985).

[17] Nicholas D. Rees, Stephen W. James and Ralph P. Tatam, Opt. Lett. **27**, 686 (2002).